

Stability Analysis of Grasped Object by Soft-Fingers based on Moment Stability

Akira Nakashima, Li Jingtai and Yoshikazu Hayakawa

Abstract—This paper analyze stability of an object grasped by a pair of soft-fingers in two-dimensional space based on moment stability. We firstly define the moment stability as a criterion for stability of a grasped object when the object is perturbed for the orientation. Based on the moment stability, the stability condition of an object grasped by a pair of hard-fingers is derived. We indicate that contact points to satisfy the condition are restricted to upper locations of the center of mass. Next, the condition of an object grasped by a pair of semispherical soft-fingers thirdly is considered. We derive a sufficient condition for the moment stability and indicate that the contact points to satisfy the condition can be in both upper and lower locations of the center of mass. Numerical examples finally are shown. An example shows the grasp situation not to satisfy the condition is established by a slender object with far lower contact locations and its grasp is stable for the faults.

I. INTRODUCTION

Many researchers have tried to introduce robots into human's daily environments. Since the robots are aimed to do various tasks instead of human, multi-fingered robot hands are effective as end-effectors. Multi-fingered robot hands have capability to grasp variously-shaped objects because the hands can grasp with multi contacts and can control grasping force via multi joint inputs.

There are many research for grasp stability of an object grasped by balanced contact forces when the object is perturbed from its equilibrium point. When the object is displaced and the balanced forces are invariant, the forces generate the resultant force and moment to the object. This is referred to as the *stiffness effect* and is a direct measure of quasi-static grasp stability [1]. Cutkosky and Kao [2] derived the stiffness matrix between resultant force/moment and small displacement of a grasped object as a function of geometry of the grasped object and contact condition. Montana [3] analyzed the stiffness effect of an grasped object with rolling contact in 2D space concerned with the curvature of the object. Maekawa et al. [4] analyzed the stiffness effect with rolling contact in 3D space and derived the stiffness matrix to evaluate the stiffness effect of the translation/rotation of the object and the contact movement due to the rolling contact. Since it is assumed that finger-tips are rigid bodies in the all studies, the stiffness effect destabilize the grasped object except for the stiffness effect due to rolling contact [4]. While these studies do not control contact forces, there are studies where the stiffness effect is controlled by contact

forces to stabilize a grasped object around its equilibrium [5], [6], [7]. In this paper, we concentrate on the stiffness effect without controlling contact forces.

Recently, soft-fingers made from soft materials has been studied. Compared with hard-fingers made from hard materials, the soft-fingers have a lot of advantages [8]: the contact friction is larger than that of the hard-finger since the contact is surface; the soft-finger can reduce the impact force in contact establishment; it can fit on varrious shapes of the object; there exists moment friction about the contact normal. Inoue et al. [9], [10] considered an one-dimensional deformation model of a semispherical soft fingertip with the geometric and material nonlinearities and proposed a quasi-static manipulation method based on the local minimum elastic energy with the rolling contact in two-dimensional space. Furthermore, they proposed a two-dimensional deformation model and studied dynamic stability [11], [12]. However, they showed the stability of the soft-finger grasp by only numerical simulations. Furthermore, since they did not decouple the contact movements due to the rolling and deformation, the stability effect of the rolling was not shown.

In this paper, we analytically study stability of an object grasped by a pair of soft-fingers in two-dimensional space based on the stiffness effect. The study [4] showed that the stiffness effect due to the object rotation is much larger than the one due to the object translation and the stiffness effect due to the rolling contact stabilize the object. Therefore, we consider the object rotation and the rolling contact. We firstly define the moment stability as a criterion for stability of a grasped object when the object is perturbed for the orientation. Based on the moment stability, the stability condition of an object grasped by a pair of hard-fingers is derived. We indicate that contact points to satisfy the condition are restricted to upper locations of the center of mass. Next, the condition of an object grasped by a pair of semispherical soft-fingers thirdly is considered. We derive a sufficient condition for the moment stability and indicate that the contact points to satisfy the condition can be in both upper and lower locations of the center of mass. Numerical examples finally are shown. An example shows the grasp situation not to satisfy the condition is established by a slender object with far lower contact locations and its grasp is stable for the faults.

II. STABILITY ANALYSIS OF HARD-FINGER GRASP

We firstly analyze stability of an object grasped by a pair of hard-fingers in 2D space as shown in Fig. 1. The object is assumed to be a convex polyhedron. Σ_O is the reference

All authors are with Mechanical Science and Engineering, Graduate School of Engineering, Nagoya University, Furo-cho, Chikusa-ku, Nagoya, Japan akira@haya.nuem.nagoya-u.ac.jp, and Y. Hayakawa is also with RIKEN-TRI Collaboration Center, RIKEN, 2271-103, Anagahora, Shimoshidami, Moriyama-ku, Nagoya, Japan.

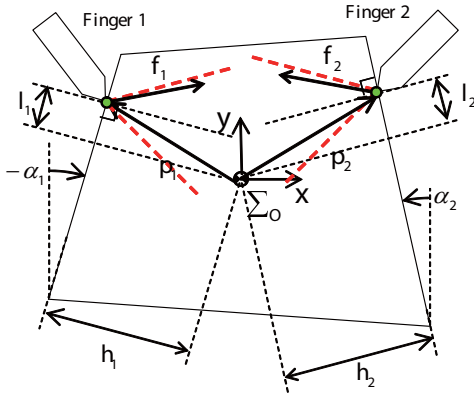


Fig. 1. An object grasped by a pair of two hard-fingers.

frame attached at the center of mass of the object. Note that vectors without left superscripts are expressed in Σ_O . $\mathbf{f}_i, \mathbf{p}_i \in \mathbb{R}^2$ ($i = 1, 2$) are the contact force and the position vector at the i th contact point respectively. l_i and h_i are the distances of the i th contact point from the center of mass along the normal and tangent, respectively. α_i is the angle of the side grasped by the i th finger from the y -axis of Σ_O . The two red thick dashed lines at the i th contact point represent the boundaries of the friction cone, which is defined as

$$\mathbf{f}_i^T \mathbf{e}_{t_i} \leq \mu_i |\mathbf{f}_i^T \mathbf{e}_{n_i}|, \quad (1)$$

where $\mathbf{e}_{n_i}, \mathbf{e}_{t_i} \in \mathbb{R}^2$ are the normal and tangent vectors and μ_i is the static friction coefficient. The grasp of the object is defined as the following equilibrium equations:

$$\mathbf{f}_1 + \mathbf{f}_2 + \begin{bmatrix} 0 \\ -mg \end{bmatrix} = 0, \quad (2)$$

$$[\mathbf{p}_1 \times] \mathbf{f}_1 + [\mathbf{p}_2 \times] \mathbf{f}_2 = 0, \quad (3)$$

where m is the mass of the object, g is the gravitational constant and $[\mathbf{p}_i \times] \in \mathbb{R}^{1 \times 2}$ is the 2D cross product defined as

$$[\mathbf{p}_i \times] := [-p_{y_i} \ p_{x_i}], \quad \mathbf{p}_i := [p_{x_i} \ p_{y_i}]^T. \quad (4)$$

For the system of the hard-finger grasp, we consider the stiffness effect due to the object rotation θ . It is assumed that the object is only rotated around the center of mass and the contact force \mathbf{f}_i is invariant. We define the *moment stability* as

$$M(\theta)\theta < 0, \quad (5)$$

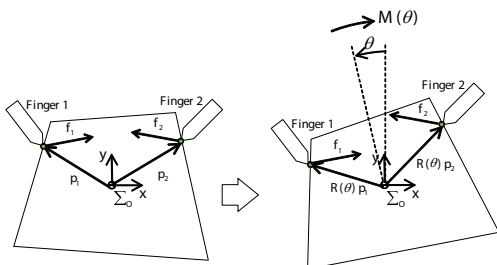


Fig. 2. Moment stability for rotation perturbation.

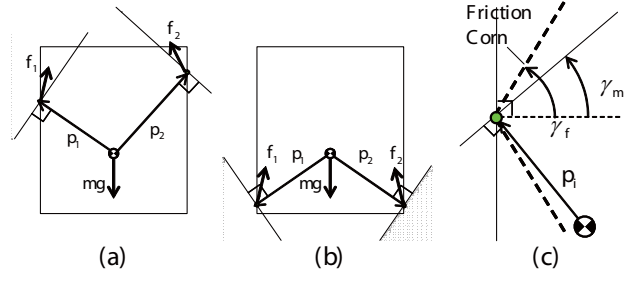


Fig. 3. Grasp situations to satisfy the sufficient condition (10).

where $M(\theta)$ is the moment caused by the object rotation θ . (5) means that $M(\theta)$ is the restoring force for the rotational displacement θ as shown in Fig. 2.

The moment $M(\theta)$ in the hard-finger grasp is given by

$$M(\theta) = [(\mathbf{R}(\theta)\mathbf{p}_1) \times] \mathbf{f}_1 + [(\mathbf{R}(\theta)\mathbf{p}_2) \times] \mathbf{f}_2, \quad (6)$$

where $\mathbf{R}(\theta) \in \mathbb{R}^{2 \times 2}$ is the rotation matrix. Calculating $[(\mathbf{R}(\theta)\mathbf{p}_i) \times]$ with (4) leads to

$$\begin{aligned} [(\mathbf{R}(\theta)\mathbf{p}_i) \times] &= [-p_{i_x} \sin \theta - p_{i_y} \cos \theta \quad p_{i_x} \cos \theta - p_{i_y} \sin \theta] \\ &= [\mathbf{p}_i \times] \mathbf{R}^T(\theta). \end{aligned} \quad (7)$$

Substituting (7) into (6), we get

$$\begin{aligned} M(\theta) &= \sum_{i=1}^2 [\mathbf{p}_i \times] \begin{bmatrix} \cos \theta & \sin \theta \\ -\sin \theta & \cos \theta \end{bmatrix} \begin{bmatrix} f_{i_x} \\ f_{i_y} \end{bmatrix} \\ &= \sum_{i=1}^2 [\mathbf{p}_i \times] \left\{ \cos \theta \begin{bmatrix} f_{i_x} \\ f_{i_y} \end{bmatrix} + \sin \theta \begin{bmatrix} f_{i_y} \\ -f_{i_x} \end{bmatrix} \right\} \\ &= \underbrace{\left(\sum_{i=1}^2 [\mathbf{p}_i \times] \mathbf{f}_i \right)}_0 \cos \theta - \left(\sum_{i=1}^2 \mathbf{p}_i^T \mathbf{f}_i \right) \sin \theta \\ &= -(\mathbf{p}_1^T \mathbf{f}_1 + \mathbf{p}_2^T \mathbf{f}_2) \sin \theta, \end{aligned} \quad (8)$$

where the first term of the third row equals 0 from (3). The following theorem holds:

Theorem 1: The necessary and sufficient condition of the moment stability for the hard-finger grasp is

$$\mathbf{p}_1^T \mathbf{f}_1 + \mathbf{p}_2^T \mathbf{f}_2 > 0. \quad (9)$$

Let us substitute the condition (9) of Theorem 1 by the following sufficient condition

$$\mathbf{p}_i^T \mathbf{f}_i > 0, \quad i = 1 \text{ and } 2. \quad (10)$$

For simplicity, the side angles are set to $\alpha_i = 0$. The areas of \mathbf{f}_1 and \mathbf{f}_2 to satisfy (10) are represented by the shaded areas in (a) and (b) of Fig. 3. It is obvious that there do not exist \mathbf{f}_1 and \mathbf{f}_2 when the contact positions are under the center of mass. In order to construct the grasp of the object, the contact force \mathbf{f}_i also has to satisfy the friction condition (1), which is illustrated in (c) of Fig. 3. γ_{f_i} and γ_{m_i} are the

angles of the boundaries of the friction cone and (10) from the contact normal, respectively. These angles are defined as

$$\gamma_{f_i} := \tan^{-1} \mu_i, \quad \gamma_{m_i} := \tan^{-1} \frac{h_i}{l_i}. \quad (11)$$

Therefore, it is necessary for the distances l_i and h_i of the contact point to satisfy

$$\gamma_{m_i} \leq \gamma_{f_i} \Leftrightarrow \frac{h_i}{l_i} \leq \mu_i \quad (12)$$

as shown in (c) of Fig. 3.

Remark 1: From (12), it is easy to grasp a slender object with the upper contact points while it is difficult to grasp a wide object with central contact points. In other words, the contact locations for the stability are restricted to far upper from the center of mass.

III. STABILITY ANALYSIS OF SOFT-FINGER GRASP

A. System Configuration

In this section, we secondly analyze stability of an object grasped by a pair of soft-fingers in 2D space. The deformation model of the soft-finger is 2D reduction model of the 3D model proposed in [13]. Fig. 4 shows the semi-spherical soft finger with the radius r_i . Σ_{F_i} is fixed at the center of the i th finger and the y_{F_i} -axis is perpendicular to the base. The deformation area of the soft-finger is defined as the dashed area, which is the overlapped area between the finger and the object. The contact point before the deformation is represented by the contact angle ϕ_i . Since the contact surface is the circle from the geometry of the deformation definition, the contact point after the deformation is defined as the center of the contact surface. In the latter, the contact point after the deformation is simply called the contact point. We define the deformation displacements δ_{r_i} and δ_{ϕ_i} as the polar coordinates of the contact point. δ_{r_i} is the radial displacement and δ_{ϕ_i} is the angle displacement in the inverse direction of ϕ_i . $\Sigma_{C_{F_i}}$ is the contact frame attached to the contact point and the x_{F_i} -axis is in the contact normal. The forces produced by the deformation are assumed to be generated based on Hook's law with respect to the small elements of the

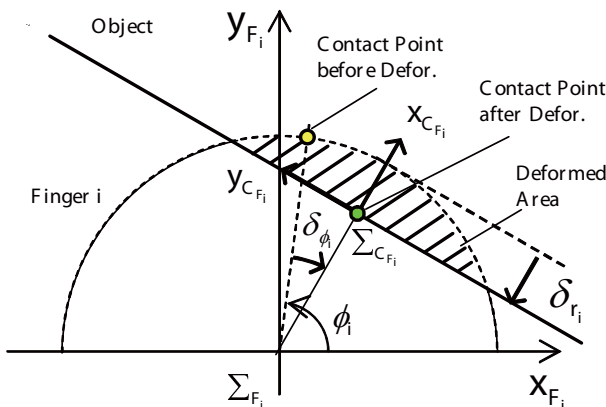


Fig. 4. Deformation model of a semi-spherical soft finger.

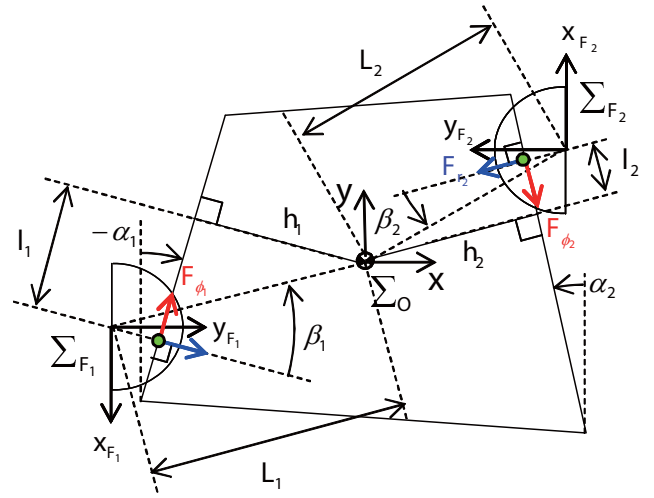


Fig. 5. An object grasped by a pair of soft-fingers.

deformation displacements. From Hook's law, the generated forces by the deformation δ_{r_i} and δ_{ϕ_i} are derived as

$$F_{r_i} := k_{r_i} \pi \delta_{r_i}^2 \quad (13)$$

$$F_{\phi_i} := \frac{2}{3} k_{\phi_i} \pi r_i^3 \frac{\delta_{\phi_i}}{\phi_i(\pi - \phi_i)} \times \frac{1}{r_i - \delta_{r_i}}, \quad (14)$$

where k_{r_i} and k_{ϕ_i} are the stiffness coefficients. The directions of F_{r_i} and F_{ϕ_i} are in $x_{C_{F_i}}$ and $y_{C_{F_i}}$ -axes, respectively. The derivation and experimental validation are shown in Appendices A and B.

Fig. 5 shows the object grasped by the soft-fingers. Note that F_{r_i} and F_{ϕ_i} are normal and tangential to the object surface. F_{r_i} and F_{ϕ_i} satisfy the following equilibrium equations:

$$\mathbf{R}_{OC_{F_1}} \mathbf{F}_1 + \mathbf{R}_{OC_{F_2}} \mathbf{F}_2 = \mathbf{0}, \quad (15)$$

$$[\mathbf{p}_1 \times] \mathbf{R}_{OC_{F_1}} \mathbf{F}_1 + [\mathbf{p}_2 \times] \mathbf{R}_{OC_{F_2}} \mathbf{F}_2 = \mathbf{0}, \quad (16)$$

where $\mathbf{F}_i := [F_{r_i} \ F_{\phi_i}]^T \in \mathbb{R}^2$, $\mathbf{R}_{OC_{F_i}} := \mathbf{R}(\theta_{F_i}) \mathbf{R}(\phi_i - \delta_{\phi_i})$, $\mathbf{R}(\theta_{F_i})$ is the rotation matrix from Σ_{F_i} to Σ_O , and $\mathbf{R}(\phi_i - \delta_{\phi_i})$ is the rotation matrix from $\Sigma_{C_{F_i}}$ to Σ_{F_i} . L_i is the length of the line segment between the centers of the i th finger and the object. β_i is the angle of this line segment from the normal to the grasped edge. These are defined as

$$\beta_i := \tan^{-1} \frac{l_i}{r_i - \delta_{r_i}(0) + h_i}, \quad (17)$$

$$L_i := \frac{r_i - \delta_{r_i}(0) + h_i}{\cos \beta_i}, \quad (18)$$

where $\delta_{r_i}(0)$ and $\delta_{\phi_i}(0)$ are the deformation displacements in the initial equilibrium grasp to satisfy (15) and (16). The other parameters and vectors are the same as in Fig. 1.

B. Rolling Contact with Deformation

The contact point ${}^{F_i} \mathbf{p}_{C_{F_i}} \in \mathbb{R}^2$ expressed in Σ_{F_i} is given by

$${}^{F_i} \mathbf{p}_{C_{F_i}} = \begin{bmatrix} (r_i - \delta_{r_i}) \cos(\phi_i - \delta_{\phi_i}) \\ (r_i - \delta_{r_i}) \sin(\phi_i - \delta_{\phi_i}) \end{bmatrix}. \quad (19)$$

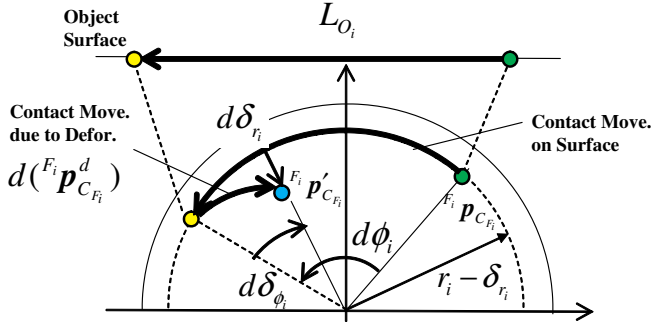


Fig. 6. Rolling motion with the deformation.

Differentiating (19) leads to

$${}^{F_i} \dot{\mathbf{p}}_{C_{F_i}}^r = {}^{F_i} \dot{\mathbf{p}}_{C_{F_i}}^r - {}^{F_i} \dot{\mathbf{p}}_{C_{F_i}}^d, \quad (20)$$

where

$${}^{F_i} \dot{\mathbf{p}}_{C_{F_i}}^r = \mathbf{R}(\phi_i - \delta_{\phi_i}) \begin{bmatrix} 0 \\ r_i - \delta_{r_i} \end{bmatrix} \dot{\phi}_i, \quad (21)$$

$${}^{F_i} \dot{\mathbf{p}}_{C_{F_i}}^d = \mathbf{R}(\phi_i - \delta_{\phi_i}) \begin{bmatrix} 1 & 0 \\ 0 & r_i - \delta_{r_i} \end{bmatrix} \begin{bmatrix} \dot{\delta}_{r_i} \\ \dot{\delta}_{\phi_i} \end{bmatrix}. \quad (22)$$

${}^{F_i} \dot{\mathbf{p}}_{C_{F_i}}^r$ represents the contact movement which is caused by the rolling of the fingertip of the radius $r_i - \delta_{r_i}$ with the rotation velocity $\dot{\phi}_i$, while ${}^{F_i} \dot{\mathbf{p}}_{C_{F_i}}^d$ represents the contact movement which is caused by the deformation movement of the fingertip with the deformation velocity $\dot{\delta}_{r_i}$ and $\dot{\delta}_{\phi_i}$. This is illustrated in Fig. 6, where ${}^{F_i} \mathbf{p}_{C_{F_i}}^d$ and ${}^{F_i} \mathbf{p}_{C_{F_i}}^r$ are the contact points before and after the contact movement, and $d\phi_i$, $d\delta_{r_i}$ and $d\delta_{\phi_i}$ are the increments of ϕ_i , δ_{r_i} and δ_{ϕ_i} respectively. The contact point ${}^{F_i} \mathbf{p}_{C_{F_i}}^d$ moves to ${}^{F_i} \mathbf{p}_{C_{F_i}}^r$ by the movements $d({}^{F_i} \mathbf{p}_{C_{F_i}}^d)$ and $d({}^{F_i} \mathbf{p}_{C_{F_i}}^d)$ due to the rolling and deformation. Since ${}^{F_i} \dot{\mathbf{p}}_{C_{F_i}}^r$ is the contact movement on the fingertip surface while ${}^{F_i} \dot{\mathbf{p}}_{C_{F_i}}^d$ is not the movement on the surface but rather the deformation movement, only ${}^{F_i} \dot{\mathbf{p}}_{C_{F_i}}^r$ equals the velocity of the contact point on the object surface:

$${}^{F_i} \dot{\mathbf{p}}_{C_{F_i}}^r = \mathbf{R}(\phi_i - \delta_{\phi_i}) \begin{bmatrix} 0 \\ \dot{L}_{O_i} \end{bmatrix}, \quad (23)$$

where the right term is the contact velocity on the object and L_{O_i} is the increment of the contact point on the object. Substituting (21) into (23), we get

$$(r_i - \delta_{r_i}) \dot{\phi}_i = \dot{L}_{O_i}. \quad (24)$$

This equation is significant to derive the deformation due to the object rotation θ in the next subsection.

C. Derivation of Moment due to Object Rotation

The moment $M(\theta)$ caused by the rotation displacement θ is derived here. From the geometric relations between the contact points and the center of mass shown in Fig. 5, $M(\theta)$ is easily given by

$$M(\theta) = M_r(\theta) + M_\phi(\theta), \quad (25)$$

where

$$M_r(\theta) := \sum_{i=1}^2 L_i \sin(\beta_i - \theta) F_{r_i}(\theta), \quad (26)$$

$$M_\phi(\theta) := \sum_{i=1}^2 -h_i F_{\phi_i}(\theta). \quad (27)$$

$M_r(\theta)$ and $M_\phi(\theta)$ are the moments generated by F_{r_i} ($i = 1, 2$) and F_{ϕ_i} ($i = 1, 2$) respectively. Since $F_{r_i}(\theta)$ and $F_{\phi_i}(\theta)$ are composed of δ_{r_i} , δ_{ϕ_i} and ϕ_i from (13) and (14), we derive δ_{r_i} , δ_{ϕ_i} and ϕ_i as functions of θ in the following.

Fig. 7 shows the geometric relation at i th contact point when the object is rotated through θ . The left and right figures show the relations before and after the rotation respectively. In the right figure, $r_{a_i}(\theta)$ is the distance of the contact point from the center of the finger. From the similar triangles with respect to the point a , $r_{a_i}(\theta)$ is obtained as

$$r_{a_i}(\theta) = L_i \cos(\beta_i - \theta) - h_i. \quad (28)$$

From (28), we get the radius deformation $\delta_{r_i}(\theta)$:

$$\delta_{r_i}(\theta) = r_i - r_{a_i}(\theta) = r_i + h_i - L_i \cos(\beta_i - \theta). \quad (29)$$

Next, we derive the rotation deformation $\delta_{\phi_i}(\theta)$ and the contact angle $\phi_i(\theta)$:

$$\delta_{\phi_i}(\theta) := \delta_{\phi_i}(0) + \Delta\delta_{\phi_i}(\theta), \quad \phi_i(\theta) := \phi_i(0) + \Delta\phi_i(\theta), \quad (30)$$

where $\Delta\delta_{\phi_i}(\theta)$ and $\Delta\phi_i(\theta)$ are the increments from the grasping equilibrium due to the rotation θ . From Fig. 7, the increment of the relative angle $\delta_{\phi_i}(\theta) - \phi_i(\theta)$ equals to θ :

$$\delta_{\phi_i}(\theta) - \phi_i(\theta) - (\delta_{\phi_i}(0) - \phi_i(0)) = \Delta\phi_i(\theta) - \Delta\delta_{\phi_i}(\theta) = \theta. \quad (31)$$

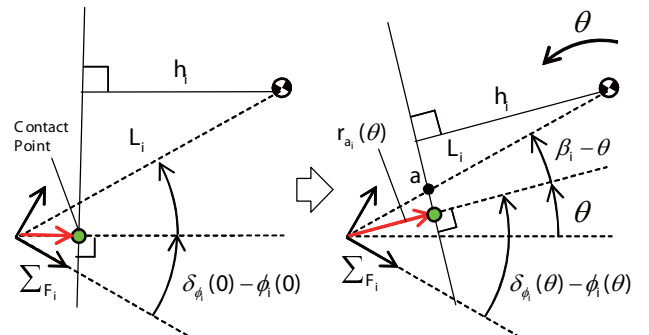
In addition to the equation (31), the following rolling contact equation holds from (24):

$$(r_i - \delta_{r_i}(\theta)) d(\Delta\phi_i(\theta)) = d(L_{O_i}(\theta)). \quad (32)$$

The contact displacement $L_{O_i}(\theta)$ on the object due to the rotation θ is obtained as

$$L_{O_i}(\theta) = L_i \sin \beta_i - L_i \sin(\beta_i - \theta), \quad (33)$$

where the first and second terms are the distances of the contact points from the center of mass along the object surface before and after the object rotation θ respectively.

Fig. 7. Geometry at the i th contact point with object rotation θ .

From the two equations (31) and (32), we can derive $\delta_{\phi_i}(\theta)$ and $\phi_i(\theta)$. From (32), (33) and (28), $d(\Delta\phi_i)$ is expressed as

$$\begin{aligned} d(\Delta\phi_i) &= \frac{L_i \cos(\beta_i - \theta)}{r_{a_i}(\theta)} d\theta = \frac{r_{a_i}(\theta) + h_i}{r_{a_i}(\theta)} d\theta \\ &= \left(1 + \frac{h_i}{r_{a_i}(\theta)}\right) d\theta. \end{aligned} \quad (34)$$

Integrating (34) from 0 to θ leads to

$$\Delta\phi_i(\theta) = \theta + \frac{h_i}{\sqrt{L_i^2 - h_i^2}}(f(0) - f(\theta)), \quad (35)$$

where

$$f(\theta) := \ln \left| \frac{\tan \frac{\beta_i - \theta}{2} + \sqrt{\frac{L_i - h_i}{L_i + h_i}}}{\tan \frac{\beta_i - \theta}{2} - \sqrt{\frac{L_i - h_i}{L_i + h_i}}} \right|. \quad (36)$$

From (31), $\delta_{\phi_i}(\theta)$ is obtained as

$$\delta_{\phi_i}(\theta) = \frac{h_i}{\sqrt{L_i^2 - h_i^2}}(f(0) - f(\theta)). \quad (37)$$

Remark 2: The deformation displacements $\delta_{r_i}(\theta)$ and $\delta_{\phi_i}(\theta)$ are derived as the functions of θ since the contact movement due to the deformation ${}^{F_i}\dot{\mathbf{p}}_{C_{F_i}}^d$ is not included in (32). If ${}^{F_i}\dot{\mathbf{p}}_{C_{F_i}}^d$ is not decoupled from (32), $\delta_{r_i}(\theta)$ and $\delta_{\phi_i}(\theta)$ can not be driven analytically.

D. Sufficient Condition of Moment Stability

We consider a condition for the moment (25) to satisfy the moment stability condition (5). The condition (5) is rewritten as

$$M(\theta)\theta = (M_r(\theta) - M_r(0))\theta + (M_\phi(\theta) - M_\phi(0))\theta < 0, \quad (38)$$

where $M_r(0) = -M_\phi(0)$ from $M(0) = 0$.

First, consider the moment $M_r(\theta)$ of (26). Since $r_{a_i}(\theta)$ of (28) is the distance of the contact point, the following inequality has to be satisfied:

$$0 < r_{a_i}(\theta) < r_i. \quad (39)$$

Substituting (28) into (39) and solving the resultant equation with respect to $\cos(\beta_i - \theta)$ lead to

$$\frac{h_i}{L_i} < \cos(\beta_i - \theta) < \frac{r_i + h_i}{L_i}. \quad (40)$$

Under the condition (40), the following lemma holds:

Lemma 1: Suppose that (40) holds. Then, the following relations hold:

$$\frac{d}{d\theta} M_r(\theta) \leq 0, \quad (M_r(\theta) - M_r(0))\theta < 0. \quad (41)$$

Proof: Differentiating (26) results in

$$\frac{dM(\theta)}{d\theta} = \frac{k_{r_i} \pi \delta_{r_i}}{3} g(\theta), \quad (42)$$

where

$$g(\theta) := \left(\cos(\beta_i - \theta) - \frac{r_i + h_i}{6L_i} \right)^2 - \left(\frac{r_i + h_i}{6L_i} \right)^2 - \frac{2}{3}. \quad (43)$$

Since $\frac{dM(\theta)}{d\theta}$ of (42) is convex downward with respect to $\cos(\beta_i - \theta)$, the maximum of $\frac{dM(\theta)}{d\theta}$ is given by the left or

right boundaries of (40). Firstly consider the case $\frac{r_i + h_i}{L_i} \leq 1$. Then,

$$\begin{aligned} g(\theta_u) &= \left(5 \frac{r_i + h_i}{6L_i}\right)^2 - \left(\frac{r_i + h_i}{6L_i}\right)^2 - \frac{2}{3} \\ &= \frac{2}{3} \left\{ \left(\frac{r_i + h_i}{L_i}\right)^2 - 1 \right\} \leq 0, \end{aligned} \quad (44)$$

$$\begin{aligned} g(\theta_l) &= \left(5 \frac{r_i + h_i}{6L_i} - \frac{r_i}{L_i}\right)^2 - \left(\frac{r_i + h_i}{6L_i}\right)^2 - \frac{2}{3} \\ &< \frac{2}{3} \left\{ \left(\frac{r_i + h_i}{L_i}\right)^2 - 1 \right\} \leq 0, \end{aligned} \quad (45)$$

where θ_u and θ_l are defined as

$$\cos(\beta_i - \theta_u) = \frac{r_i + h_i}{L_i}, \quad \cos(\beta_i - \theta_l) = \frac{h_i}{L_i}.$$

Next consider the case $\frac{r_i + h_i}{L_i} > 1$. Then, $g(\theta_u)$ takes the different value given by

$$g(\theta_u) = \frac{L_i - (r_i + h_i)}{3L_i} < 0, \quad (46)$$

where θ_u is defined as

$$\cos(\beta_i - \theta_u) = 1.$$

The maximum of $g(\theta)$ is one of (44), (45) and (46). Therefore, from (42), (43), (41) holds. ■

Remark 3: Lemma 1 indicates that the moment produced by the radius forces $F_{r_i}(\theta)$ ($i = 1, 2$) always effects on the restoring force to stabilize the object against the rotational perturbation.

Second, consider the moment $M_\phi(\theta)$ of (27). Substituting the following formula of trigonometric functions

$$\cos(\beta_i - \theta) = \frac{1 - \tan^2 \frac{\beta_i - \theta}{2}}{1 + \tan^2 \frac{\beta_i - \theta}{2}}$$

into (40) and solving the resultant inequality with respect to $\tan \frac{\beta_i - \theta}{2}$ yield

$$\left| \tan \frac{\beta_i - \theta}{2} \right| < \sqrt{\frac{L_i - h_i}{L_i + h_i}}. \quad (47)$$

Under the condition (47), the following lemma holds:

Lemma 2: Suppose that (47) holds. Then, $\Delta\phi_i(\theta)$ and $\Delta\delta_{\phi_i}(\theta)$ of (35) and (37) are monotone increasing.

Proof: From (35) and (37), it is sufficient to check the property of $f(\theta)$ of (36). $f(\theta)$ is rewritten as

$$f(\theta) = \ln f_1(f_2(\theta)), \quad (48)$$

where

$$f_1(x) := \left| \frac{x + a_i}{x - a_i} \right|, \quad a_i := \sqrt{\frac{L_i - h_i}{L_i + h_i}} \quad (49)$$

$$f_2(x) := \tan \frac{\beta_i - \theta}{2}. \quad (50)$$

As for the function $f_1(x)$,

$$\left(\frac{x + a_i}{x - a_i} \right)' = \frac{-2a_i}{(x - a_i)^2} < 0, \quad f(-a_i) = 0.$$

Therefore, $f_1(x) > 0$ and $f_1'(x) > 0$ in the case $|x| < a_i$ from (47). On the other hand, the function $f_2(x)$ is monotone decreasing because

$$\left(\tan \frac{\beta_i - x}{2} \right)' = -\frac{1}{2 \cos^2 \frac{\beta_i - x}{2}} < 0.$$

Furthermore, $|f_2(x)| < a_i$ from (47). Since $f_1(f_2(\theta))$ is monotone decreasing and $\ln x$ is monotone increasing, $f(\theta)$ is monotone decreasing. Therefore, $\Delta\phi_i(\theta)$ and $\Delta\delta_{\phi_i}(\theta)$ of (35) and (37) are monotone increasing because $\Delta\phi_i(\theta)$ and $\Delta\delta_{\phi_i}(\theta)$ have $-f(\theta)$. ■

A sufficient condition for the moment (25) to satisfy the moment stability condition (5) is derived:

Theorem 2: Suppose that

$$\delta_{\phi_i} \{ (2\phi_i - \pi)(r_{a_i} + h_i) - L_i \sin(\beta_i - \theta) \phi_i (\pi - \phi) \} + \phi_i (\pi - \phi_i) h_i > 0. \quad (51)$$

Then, (5) holds.

Proof: From (14), differentiating $F_{\phi_i}(\theta)$ leads to

$$\begin{aligned} \frac{d}{d\theta} F_{\phi_i}(\theta) &= \frac{2}{3} k_{\phi} \pi r_i^3 \times \frac{1}{\{r_{a_i} \phi_i (\pi - \phi_i)\}^2} \times \\ &\left\{ \delta_{\phi_i} (2\phi - \pi)(r_{a_i} + h_i) + \right. \\ &\left. \phi_i (\pi - \phi_i) \{ h_i - L_i \delta_{\phi_i} \sin(\beta_i - \theta) \} \right\}. \quad (52) \end{aligned}$$

From (52) and (51), the following holds:

$$\frac{d}{d\theta} F_{\phi}(\theta) > 0. \quad (53)$$

From (27), (53) yields to

$$(M_{\phi}(\theta) - M_{\phi}(0))\theta < 0. \quad (54)$$

Therefore, from (38) and Lemma 1, (5) holds. ■

Remark 4: The next section shows an example not to hold the condition (51). However, the grasped object is stable since the moment produced by the radius forces $F_{r_i}(\theta)$ ($i = 1, 2$) are much larger than the moment produced by the rotation forces $F_{\phi_i}(\theta)$ ($i = 1, 2$). The grasp situation of the shown example is similar. This can imply that the condition (51) can hold in ordinary cases of grasping.

IV. NUMERICAL EXAMPLES

Numerical examples are shown to confirm the stability of the soft-finger grasp.

Fig. 8 (a) shows the case where the rectangular object is grasped at the upper contact points. The radius of the finger is $r_i = 10$ [mm] and the coefficients are $k_{r_i} = 0.377$, $k_{\phi_i} = 0.166$ [N/mm²] as shown in Appendix B. The height, width and mass of the object are 120, 100[mm] and $m = 0.3$ [kg] respectively. The distances of the i th contact point from the center of mass are $l_i = 50$ and $h_i = 50$ [mm]. The contact angles are $\phi_1 = \phi_2 = 90$ [deg]. The initial deformation displacements are $\delta_{r_1}(0) = \delta_{r_2}(0) = 2$ [mm] and $\delta_{\phi_1}(0) = -\delta_{\phi_2}(0) = 10$ [deg]. From these parameters, (17) and (18), $\beta_1 = -\beta_2 = 41$ [deg] and $L_1 = L_2 = 76.5$ [mm]. The parameters satisfy the condition (51). Fig. 8 (a) shows the

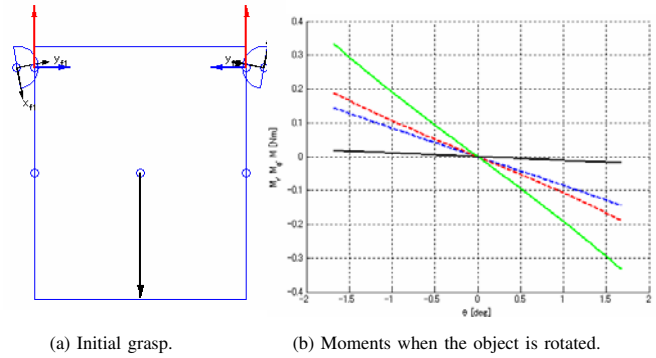


Fig. 8. Numerical example 1.

initial situation of the grasping. The red, blue and black arrows are the radial forces F_{r_i} , rotational forces F_{ϕ_i} and gravity force mg respectively. Fig. 8 (b) shows the moments $M_r(\theta)$, $M_{\phi}(\theta)$, $M(\theta)$ and $M_h(\theta)$, which are dashed blue line, red line, solid green line and black line, respectively. $M_h(\theta)$ is the moment in the case of the hard-finger grasp, which is defined as (8). Note that the black line represents $M_h(\theta) \times 10$. We confirm that the all moments are the restoring forces and $M(\theta)$ is much larger than $M_h(\theta)$. This shows that the stability of the soft-finger grasp is much better than that of the hard-finger grasp. Note that the range of θ is given by the product set of the ranges of θ to satisfy (40), $-\pi < \delta_{\phi_i}(\theta) < \pi$ and $0 < \phi_i(\theta) < \pi$ with (30), (35)–(37). Fig. 9 shows F_{r_i} and F_{ϕ_i} when the object is rotated in the positive and negative directions. In the case $\theta > 0$, the forces F_{r_1} and F_{ϕ_1} to stabilize the object increase while the forces F_{r_2} and F_{ϕ_2} to destabilize the object decrease. This indicate that the forces produced by the soft-finger deformation effect on the stability well. The case $\theta < 0$ is similar to the case $\theta > 0$.

Figs. 10-11 show the case where the object is grasped at the lower contact points. The parameters and definitions of the arrows and lines are the same as Figs. 8-9. In Fig. 10 (a), we confirm that the moments M_r , M_{ϕ} and M are the restoring forces while the moment M_h destabilizes the grasped object. This shows that the soft-finger grasp is stable even when the hard-finger grasp is unstable. In the case $\theta > 0$ of Fig. 11, the forces F_{r_2} and F_{ϕ_1} to stabilize the

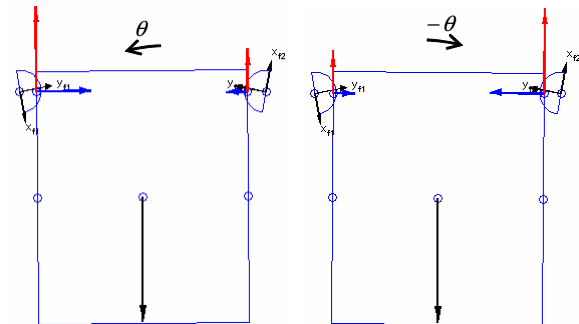


Fig. 9. F_{r_i} and F_{ϕ_i} of the example 1 when the object is rotated.

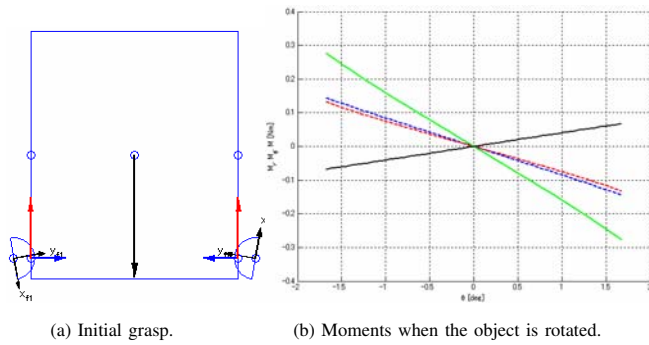


Fig. 10. Numerical example 2.

object increase while the forces F_{r_1} and F_{ϕ_2} to destabilize the object decrease. This indicates that the forces produced by the soft-finger deformation effect on the stability although the contact locations are changed. The case $\theta < 0$ is similar to the case $\theta > 0$.

Let us consider a situation not to satisfy the sufficient condition (51). In the condition (51), it is obvious that $r_{a_i} + h_i > 0$ and $\phi_i(\pi - \phi_i) > 0$ from (39) and $0 < \phi_i < \pi$. Therefore, the following conditions have to hold not to satisfy (51):

$$\delta_{\phi_i} > 0 : 2\phi_i - \pi < 0, \sin(\beta_i - \theta) > 0, \quad (55)$$

$$\delta_{\phi_i} < 0 : 2\phi_i - \pi > 0, \sin(\beta_i - \theta) < 0. \quad (56)$$

(55) and (56) lead to

$$\delta_{\phi_i} > 0 : \phi_i \ll 1, \beta_i \gg 1, \quad (57)$$

$$\delta_{\phi_i} < 0 : \phi_i \gg 1, \beta_i \ll -1. \quad (58)$$

In the initial grasp, $\delta_{\phi_1} > 0$ and $\delta_{\phi_2} < 0$. Therefore, (57) and (58) correspond to $i = 1$ and $i = 2$ respectively. In order to achieve (57) and (58), the object with the height 192[mm] and width 20[mm] is grasped. The distances of the lower i th contact point from the center of mass are $l_i = 80$ and $h_i = 10$ [mm]. The contact angles are $\phi_1 = 30$ and $\phi_2 = 150$ [deg]. The initial deformation displacements are $\delta_{r_1}(0) = \delta_{r_2}(0) = 2$ [mm] and $\delta_{\phi_1}(0) = -\delta_{\phi_2}(0) = 6$ [deg]. From these parameters, $\beta_1 = -\beta_2 = 77$ [deg] and $L_1 = L_2 = 81.2$ [mm]. Fig. 12 (a) shows the initial grasp and Fig. 12 (b) shows the moments when the object is rotated. Note that the dashed red line represents $M_\phi(\theta) \times 100$. We

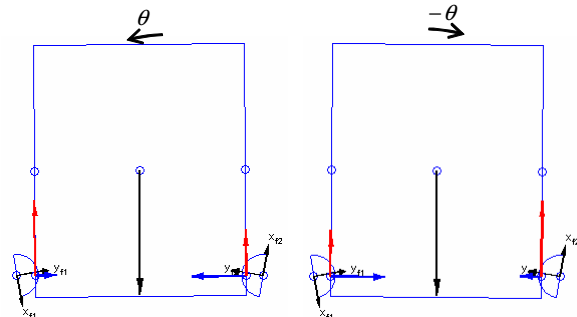
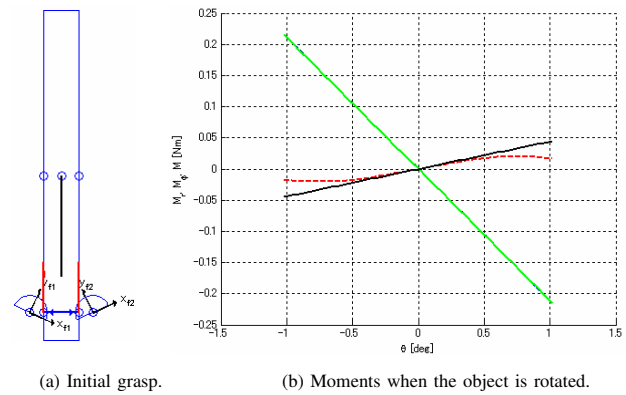
Fig. 11. F_{r_2} and F_{ϕ_i} of the example 2 when the object is rotated.

Fig. 12. Numerical example 3.

confirm that the moment $M(\theta)$ stabilizes the object while the moment $M_\phi(\theta)$ produced by F_{ϕ_i} destabilizes the object. This is because the moment produced by F_{r_i} is much larger than the moment M_ϕ . Note that the condition $\delta_{\phi_i} > 0$ (< 0) of (55) or (56) is broken when the rotation displacement θ decreases (increases) because $\delta_{\phi_i}(\theta)$ is monotone increasing from Lemma 2. Therefore, F_{ϕ_1} or F_{ϕ_2} can satisfy the condition (51). This result indicates that the grasping situation not to satisfy (51) is composed of only particular the shape of the object, contact points and contact angles and in that situation the soft-finger grasp also is stable.

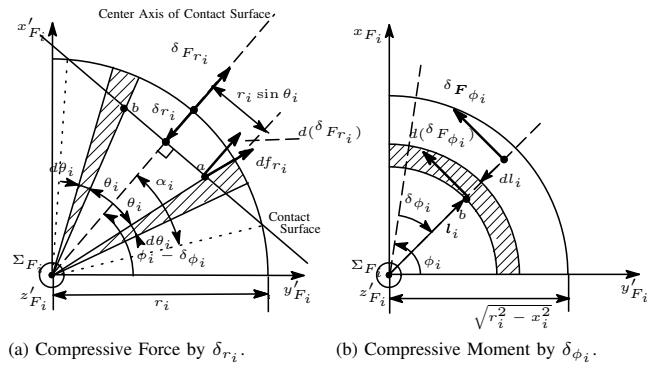
V. CONCLUSIONS AND FUTURE WORKS

This paper analyzed stability of an object grasped by a pair of soft-fingers in two-dimensional space based on moment stability. We firstly defined the moment stability as a criterion for stability of a grasped object when the object is perturbed for the orientation. Based on the moment stability, the stability condition of an object grasped by a pair of hard-fingers was derived. We indicated that contact points to satisfy the condition are restricted to upper locations of the center of mass. Next, the condition of an object grasped by a pair of semispherical soft-fingers thirdly was considered. We derived a sufficient condition for the moment stability and indicated that the contact points to satisfy the condition can be in both upper and lower locations of the center of mass. Numerical examples finally were shown. An example shows the grasp situation not to satisfy the condition is established by a slender object with far lower contact locations and its grasp is stable for the faults.

In future works, it is necessary to consider the friction condition and the limitation of finger joints. We will try to optimize the soft-finger grasp with respect to the mentioned conditions.

REFERENCES

- [1] M. T. Mason and J. K. Salisbury, *Robot Hands and the Mechanics of Manipulation*, Cambridge, MA: MIT Press, 1985.
- [2] M. Cutkosky and I. Kao: Computing and Controlling the Compliance of a Robot Hand, *IEEE Trans. Robot. Automat.*, Vol. 5, No. 2, pp. 151-165, 1989.
- [3] D. J. Montana: Contact Stability for Two-Fingered Grasps, *IEEE Trans. Robot. Automat.*, Vol. 8, No. 4, pp. 421-430, 1992.

Fig. 13. Finger-tip forces by δr_i and $\delta \phi_i$.

- [4] H. Maekawa, K. Tanie and K. Komoriya, Kinematics, Statics and Stiffness Effect of 3D Grasp by Multifingered Hand with Rolling Contact at the Fingertip, Proc. of Int. Conf. on Robot. Automat., pp. 78-85, 1997.
- [5] M. Kaneko, N. Imamura, K. Yokoi and K. Tanie, A Realization of Stable Grasp Based on Virtual Stiffness Model by Robot Fingers, IEEE Int. Workshop on Advanced Motion Control, pp.156-163, 1990.
- [6] H. Maekawa, K. Tanie, K. Komoriya and M. Kaneko, Stable Grasp and Manipulation of an Object by a Three-Fingered Hand Using Position and Stiffness Control, Proc. of Int. Conf. on Robot. Automat., 1995.
- [7] Y. Funahashi, T. Yamada, M. Tate and Y. Suzuki, Grasp stability analysis considering the curvatures at contact points, Proc. Int. Conf. Robot. Automat., pp. 3040-3046, 1996.
- [8] K. B. Shimoga and A. A. Goldenberg: Soft Robotic Fingertips Part I: A Comparison of Construction Materials, *Int. J. Robot. Res.*, Vol. 15, No. 4, 320-334, 1996.
- [9] T. Inoue and S. Hirai, "Elastic Model of Deformable Fingertip for Soft-fingered Manipulation," *IEEE Trans. on Robotics*, vol. 22, no. 6, pp. 1273-1279, 2006.
- [10] T. Inoue and S. Hirai, Quasi-Static Manipulation with Hemispherical Soft Fingertip via Two Rotational Fingers, Proc. Int. Conf. on Robot. Automat., pp.1947-1952, 2005.
- [11] T. Inoue and S. Hirai, Study on Hemispherical Soft-Fingered Handling for Fine Manipulation by Minimum D.O.F. Robotic Hand, Proc. Int. Conf. on Robot. Automat., pp.2454-2459, 2006.
- [12] T. Inoue and S. Hirai, Dynamic Stable Manipulation via Soft-Fingered Hand, Proc. Int. Conf. on Robot. Automat., pp.586-591, 2007.
- [13] A. Nakashima, T. Shibata and Y. Hayakawa, "Grasp and manipulation by soft finger with 3-dimensional deformation," Int. Conf. on Mechatronics and Information Technology, 2007.

APPENDIX

A. Derivation of Forces by Deformation

(1) Derivation of δF_{r_i} :

Consider the dashed area of the small element db_i rotated about the center axis of the contact surface through $d\psi_i$ in Fig. 13 (a). df_{r_i} is the force generated by the deformation at the point a . Since the force parallel to the contact surface $df_{r_i} \sin \theta_i$ is counteractive against $-df_{r_i} \sin \theta_i$ at the symmetric point b of a with respect to the center axis, it is sufficient to consider forces in the center axis $df_{r_i} \cos \theta_i$. Since the compression ratio at a is $1 - \frac{r_i - \delta r_i}{r_i \cos \theta_i}$, the generated force $d(\delta F_{r_i})$ of the small area at a is given by $d(\delta F_{r_i}) = 2 \times k_{r_i} \left(1 - \frac{r_i - \delta r_i}{r_i \cos \theta_i}\right) r_i d\theta_i r_i \sin \theta_i d\psi_i \times \cos \theta_i$, where k_{r_i} is the stiffness coefficient. Then,

$$\begin{aligned} \delta F_{r_i} &= \int_0^{\alpha_i} \int_0^{\pi} 2k_{r_i} \left(1 - \frac{r_i - \delta r_i}{r_i \cos \theta_i}\right) r_i^2 \sin \theta_i \cos \theta_i d\psi_i d\theta_i \\ &= \pi k_{r_i} \delta r_i^2, \end{aligned} \quad (59)$$

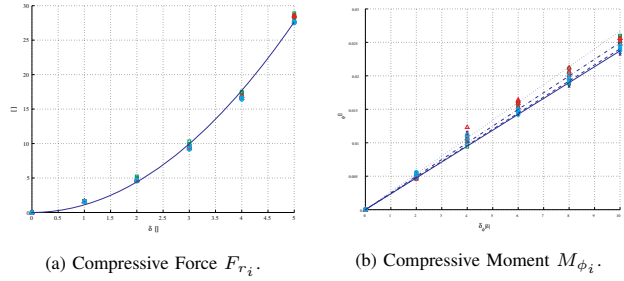


Fig. 14. Experimental validation of the force model.

where $\alpha_i := \arccos\left(\frac{r_i - \delta r_i}{r_i}\right)$.

(2) Derivation of δF_{ϕ_i} :

Fig. 13 (b) shows the cross section such that the cross section of Fig. 13 (a) is moved along z'_{F_i} -axis with the distance z_i . Consider the dashed area of the small element dl_i with the width dz_i . Since the compression ratios of the compressive and extensive directions are $\frac{\delta \phi_i}{\phi_i}$ and $\frac{\delta \phi_i}{\pi - \phi_i}$, the generated moment of the dashed area is given by $d(M_{\phi_i}) = l_i \times k_{\phi_i} \left(\frac{\delta \phi_i}{\pi - \phi_i} + \frac{\delta \phi_i}{\phi_i}\right) dl_i dz_i$, where k_{ϕ_i} is the stiffness coefficient. Then,

$$\begin{aligned} M_{\phi_i} &= \int_{-r_i}^{r_i} \int_0^{\sqrt{r_i^2 - z_i^2}} l_i k_{\phi_i} \left(\frac{\delta \phi_i}{\pi - \phi_i} + \frac{\delta \phi_i}{\phi_i}\right) dl_i dz_i \\ &= \frac{2}{3} k_{\phi_i} r_i^3 \left(\frac{1}{\pi - \phi_i} + \frac{1}{\phi_i}\right) \delta \phi_i. \end{aligned} \quad (60)$$

Since the point of application of the moment M_{ϕ_i} is the contact point with the length $r_i - \delta r_i$ from the center of the finger, the force produced by rotational deformation $\delta \phi_i$ is given by

$$F_{\phi_i} := \frac{M_{\phi_i}}{r_i - \delta r_i}. \quad (61)$$

B. Experimental validation of the force model

The material of the soft fingers is an urethane resin with the hardness C-5. The radius of the soft-finger is 10[mm]. Fig. 14 show the experimental results of F_{r_i} and F_{ϕ_i} of (13) and (14). The stiffness coefficients in (13) and (14) are calculated by the least-squares method with the force model of (13) and (14) and the experimental data. The coefficients are $k_{r_i} = 0.377$, $k_{\phi_i} = 0.166[\text{N}/\text{mm}^2]$. The lines represent the force model of (13) and (14) with the estimated coefficients. In Fig. 14 (a), the cross, square, triangle and circle represent the forces of F_{r_i} with $\phi_i = 90, 80, 70$ and $60[\text{deg}]$ respectively. In Fig. 14 (b), the solid, dashed, dashed and single-dotted and dotted lines correspond to the experimental data with the cross, square, triangle and circle which are the same as Fig. 14 (a). In Fig. 14 (a) and (b), we confirm that the lines are approximate to the experimental data.